Electronic Supplementary Material (ESI) for Journal of Materials Chemistry A.

Supporting information

Surface functionalized UiO-66/Pebax-based ultrathin composite hollow fiber gas separation membranes

Putu Doddy Sutrisna[1], Jingwei Hou[1,2*], Muhammad Yazid Zulkifli[1], Hongyu Li[1], Yatao Zhang[3], Weibin Liang[4], Deanna M. D'Alessandro[4] and Vicki Chen[1]

[1]UNESCO Centre for Membrane Science and Technology, School of Chemical Engineering, University of New South Wales, Sydney, NSW 2052, Australia

[2]Department of Materials Science and Metallurgy, University of Cambridge, CB3 0FS, Cambridge, UK

[3]School of Chemical Engineering and Energy, Zhengzhou University, Zhengzhou 450001, PR China

[4]School of Chemistry, The University of Sydney, Sydney, NSW 2006, Australia

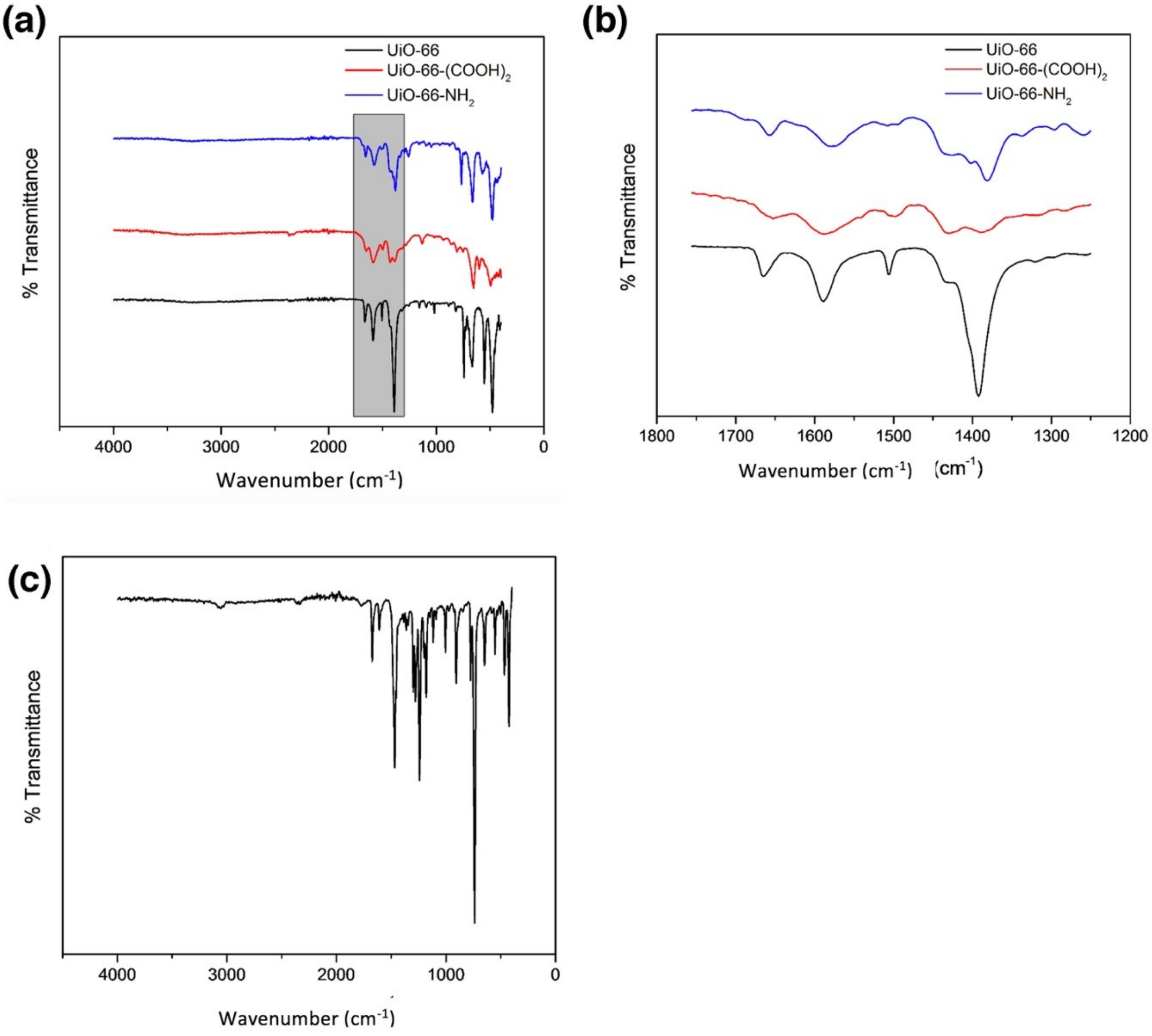

Fig. S1. FTIR spectra of (a-b) UiO-66 particles and (c) ZIF-7 particles.

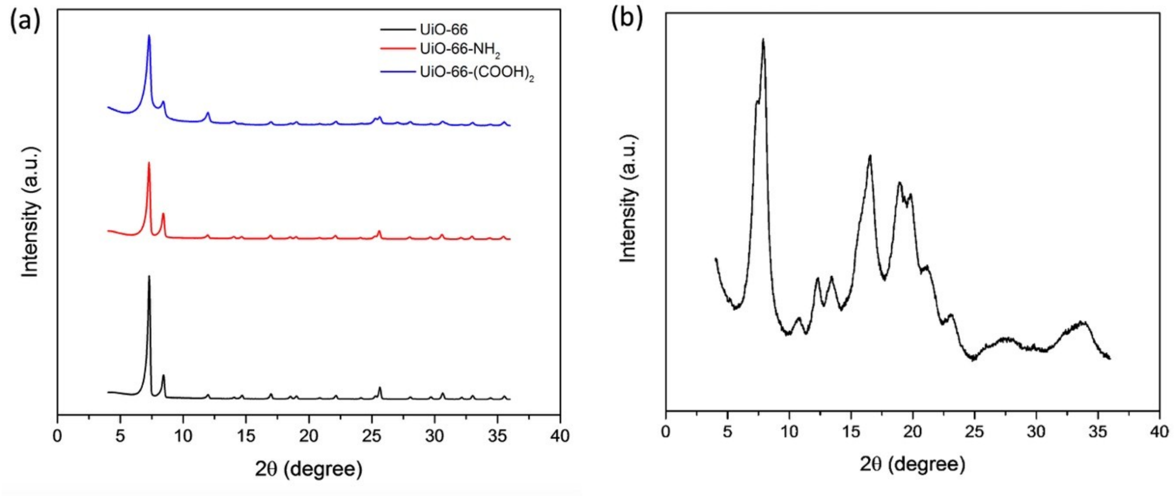

Fig. S2. XRD patterns of (a) different UiO-66 particles and (b) ZIF-7 particles.

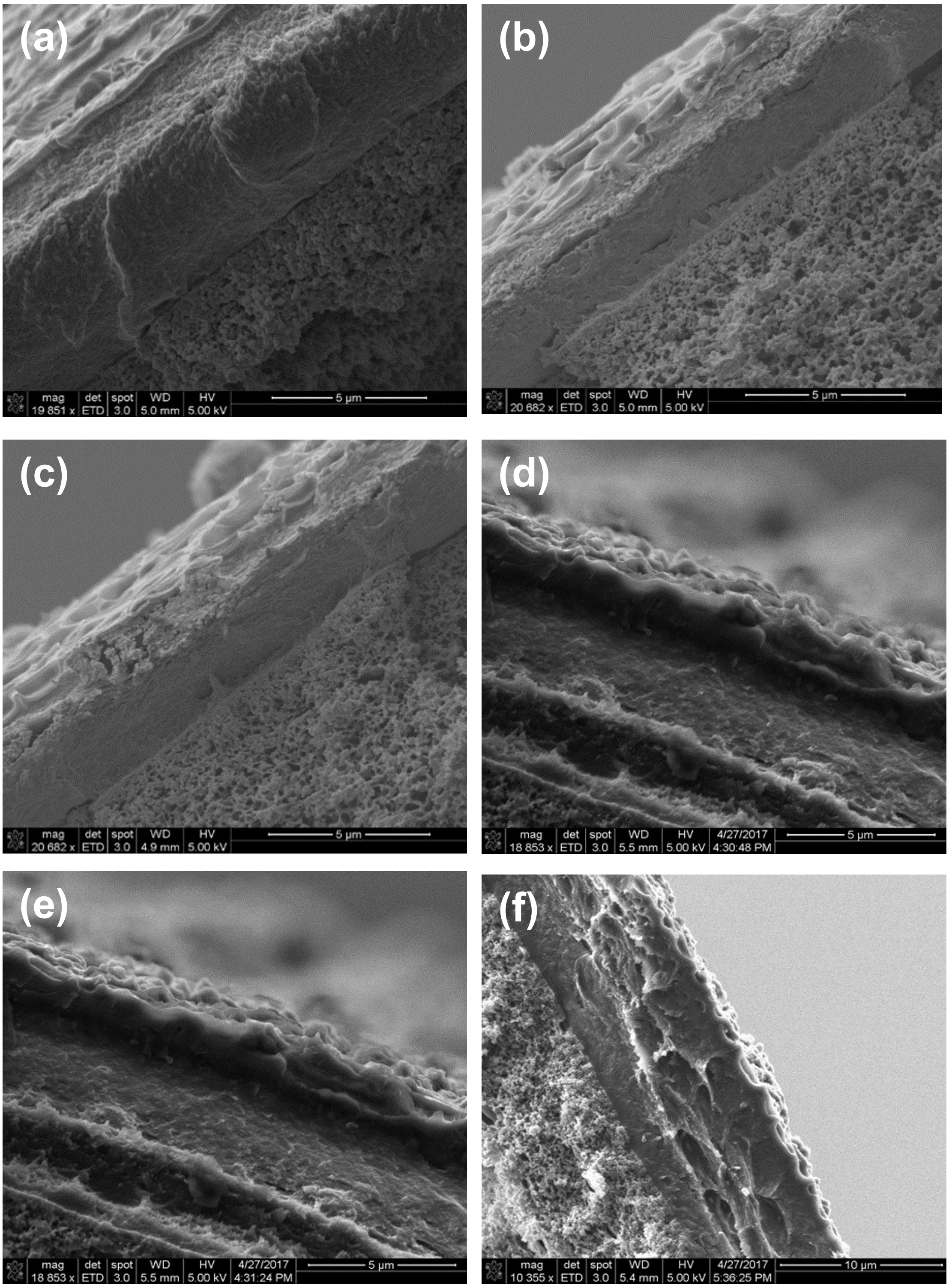

Fig.S3. Cross-sectional SEM images of composite membranes with different coating layers: (a) PTMSP and 10 wt% UiO-66 in Pebax, (b) PTMSP and 10 wt% UiO-66-NH_2 in Pebax, (c) PTMSP and 10 wt% UiO-66-$(COOH)_2$ in Pebax, (d) PTMSP and 30 wt% UiO-66 in Pebax, (e) PTMSP and 30 wt% UiO-66-NH_2 in Pebax and (f) PTMSP and 30 wt% UiO-66-$(COOH)_2$. All membranes have an extra Pebax protective layer.

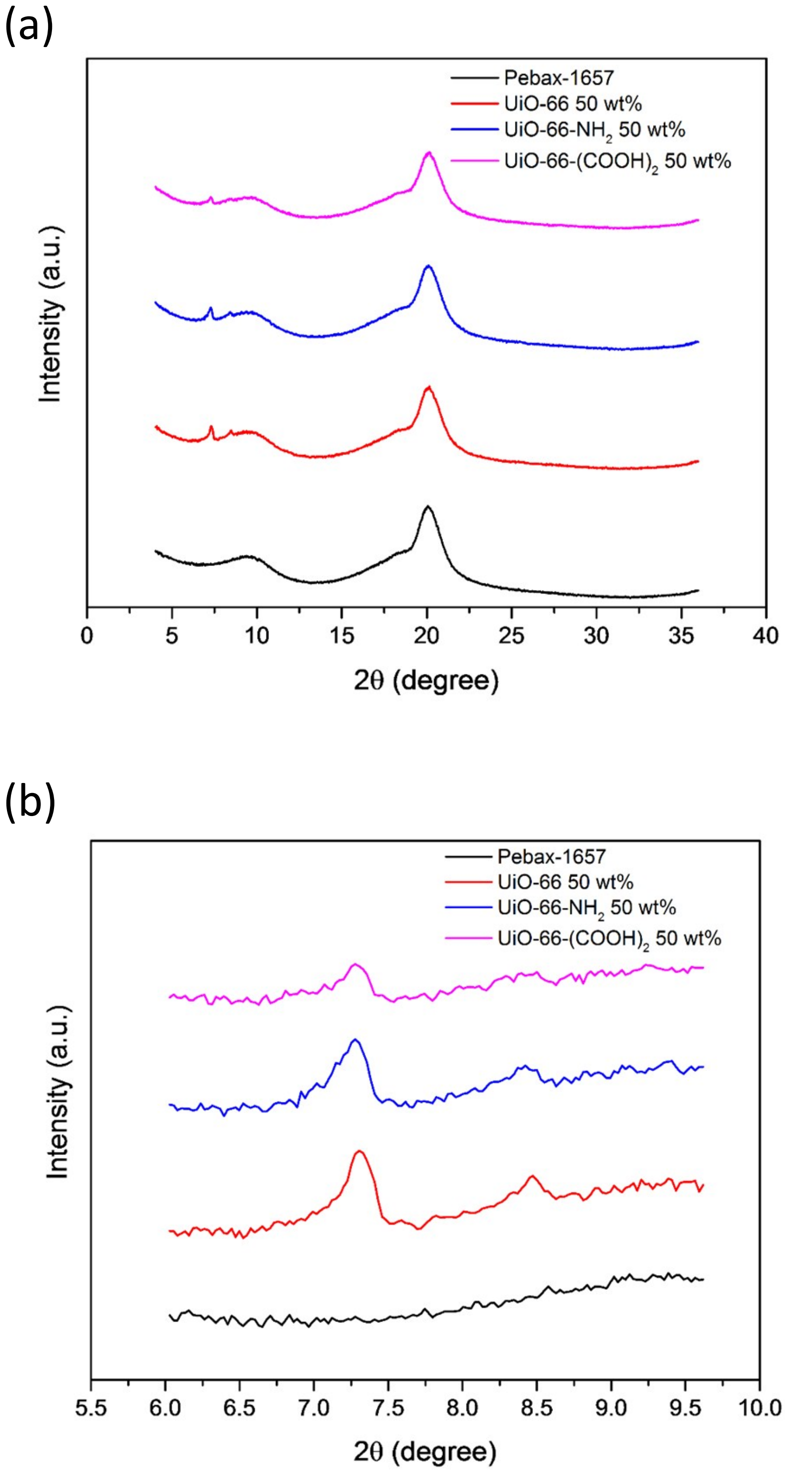

Fig.S4. XRD patterns of different UiO-66/Pebax-1657-based nanocomposite membranes at 2θ range: (a) from 4° to 36° and (b) from 6° to 9.5°

Table S1 Comparison of hollow fibre membranes only with gutter layer coatings.

	Gas permeance (GPU)			**Gas selectivity**	
	N_2	**CH_4**	**CO_2**	**CO_2/N_2**	**CO_2/CH_4**
Four layers of PDMS	1523.5	3487.7	1820.7	1.2	0.52
Four layers of PTMSP	373.8	830.8	2440.1	6.5	2.9

In this work, the Maxwell model was applied to predict CO_2 permeability and CO_2/N_2 selectivity of UiO-66/Pebax composite membranes. Due to the lack of the theoretical performance data for UiO-66-NH_2, and UiO66-$(COOH)_2$, only pristine UiO-66 was examined here. Some of the model parameters are: the density of UiO-66 particle is 1.2 g/cm^3; the thickness of the selective is based on the EDX and SEM images, and for the composite membrane with clear nanoparticle aggregations, only the bottom section thickness is calculated; and the overall membrane performance is dominated by the selective layers.

The experimental results on gas separation performance of pristine UiO-66/Pebax composite membranes were compared with ideal Maxwell model represented by equation:

$$P_{mm} = P_c\left(\frac{P_d + 2P_c - 2\emptyset_d(P_c - P_d)}{P_d + 2P_c + \emptyset_d(P_c - P_d)}\right)$$

where P_{mm} is the effective permeability of a mixed matrix UiO-66/Pebax, Φ is UiO-66 particle volume fraction, while c and d denote the continuous (Pebax polymer) and dispersed phases (UiO-66 particles), respectively. Fig.S5 presented the comparison between ideal Maxwell model and experimental results of pristine UiO-66/Pebax based membranes in this work. The Maxwell model predicts an increase in gas permeance and a decrease in CO_2/N_2 selectivity with higher particle loading, and these results are not well aligned with the experimental data. The difference between composite membrane performance data and the theoretical Maxwell model can be attributed to the following reasons below: 1) for our composite membrane, it is challenging to accurately determine the exact thickness of the Pebax/MOFs selective layer due to the interfusion of the selective layer and the gutter layer (as shown in the SEM images of Fig.6 in the manuscript); 2) the thin polymeric section may have different performance when compared with the theoretical material permeability due to the microphase separation; 3) the Maxwell model does not consider the interaction between polymeric matrix and nanofillers. In our case, the hydrogen bonding between UiO-66 and Pebax can rigidify the polymeric chains, which may change the gas transport behaviour for the polymeric sections; and 4) the Maxwell assume nanofillers are evenly dispersed within the matrix. But for our composite membrane, the high loading of UiO-66 can clearly lead to its aggregation and this can inevitably change the membrane performance.

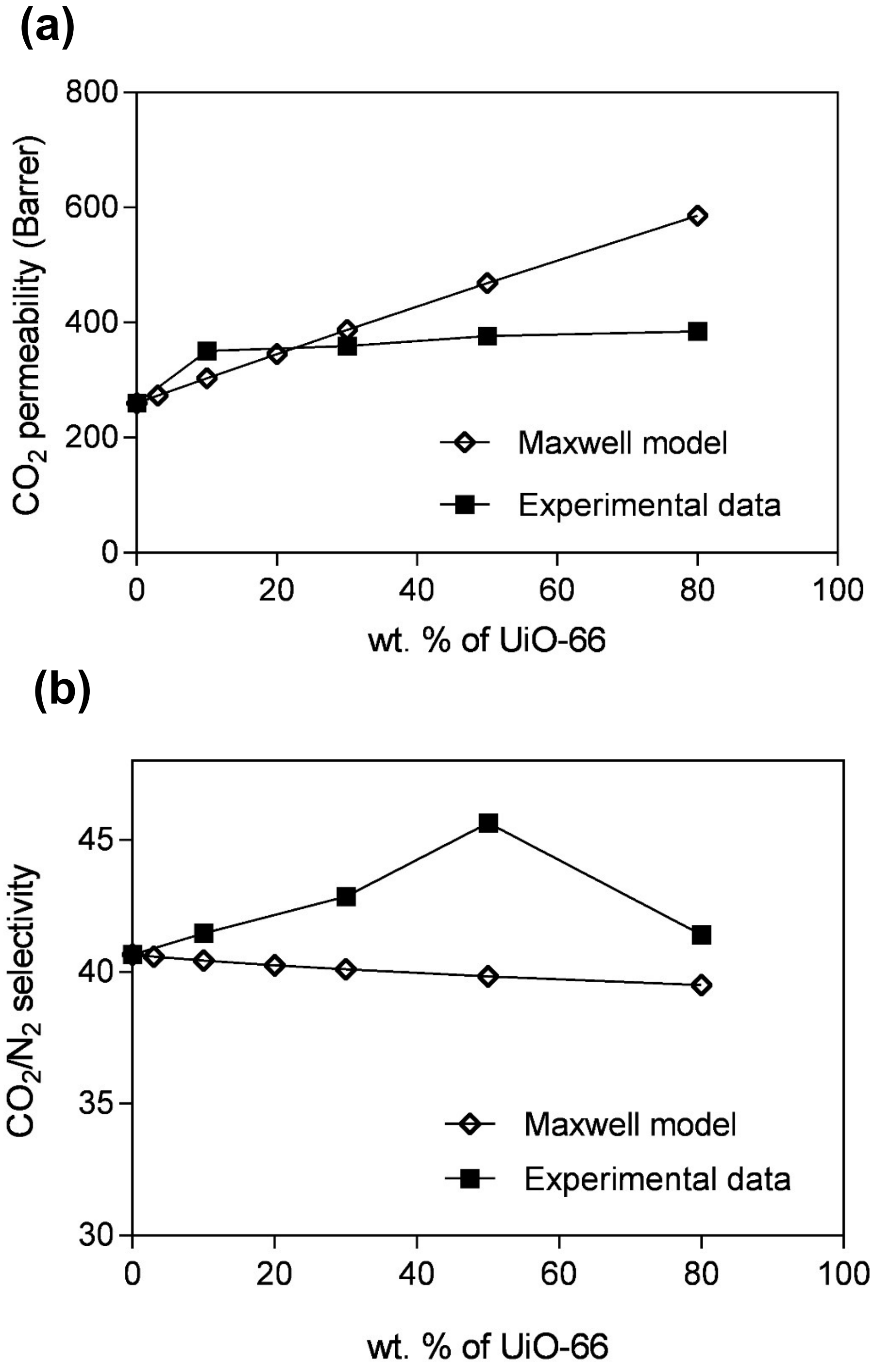

Fig.S5. Comparison between Maxwell model and experimental results of pure UiO-66/Pebax-based composite membranes: (a) CO_2 permeability and (b) CO_2/N_2 selectivity.

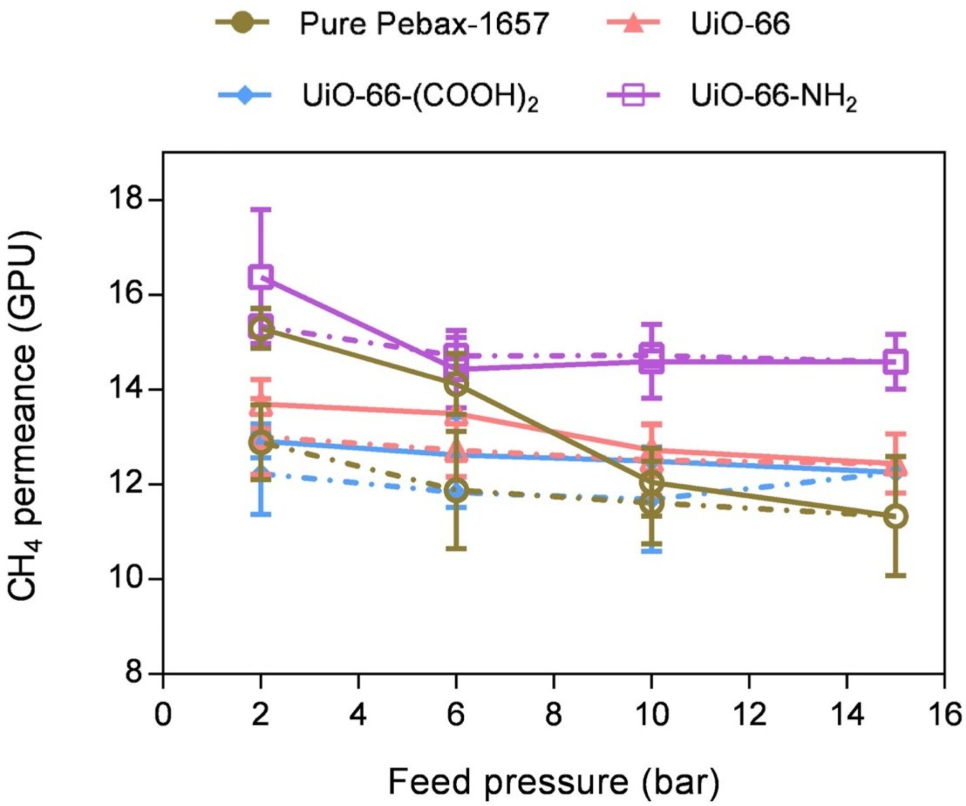

Fig.S6. The effect of feed pressure on CH_4 permeance for various UiO-66/Pebax-1657-based composite membranes (solid line represents pressurization step and dash line represents depressurization step).

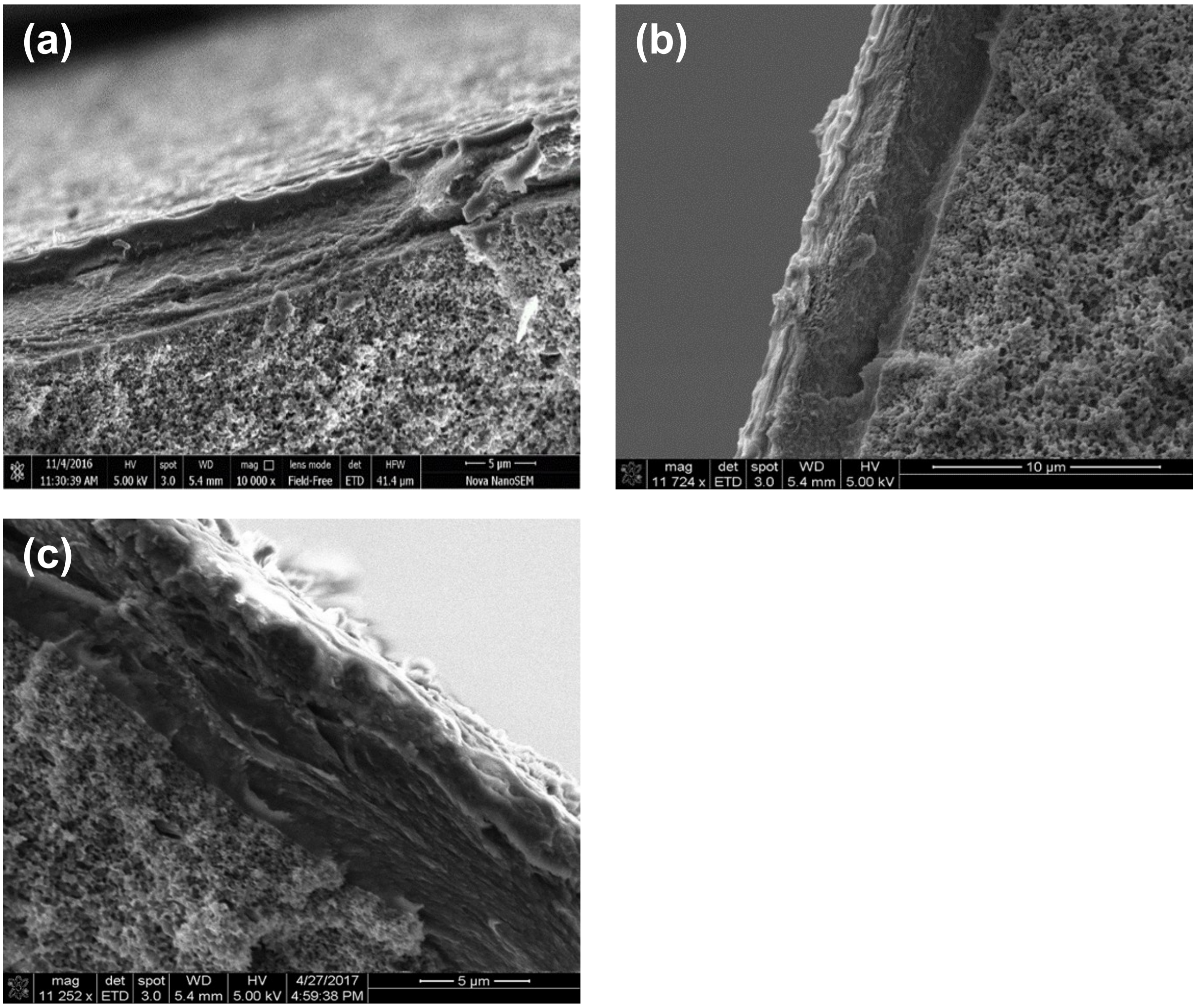

Fig.S7. Cross-sectional SEM images of composite membranes with different coating layers: (a) PTMSP and 10 wt% ZIF-7 in Pebax, (b) PTMSP and 20 wt% ZIF-7 in Pebax, (c) PTMSP and 30 wt% ZIF-7 in Pebax. All membranes have an extra Pebax protective layer.

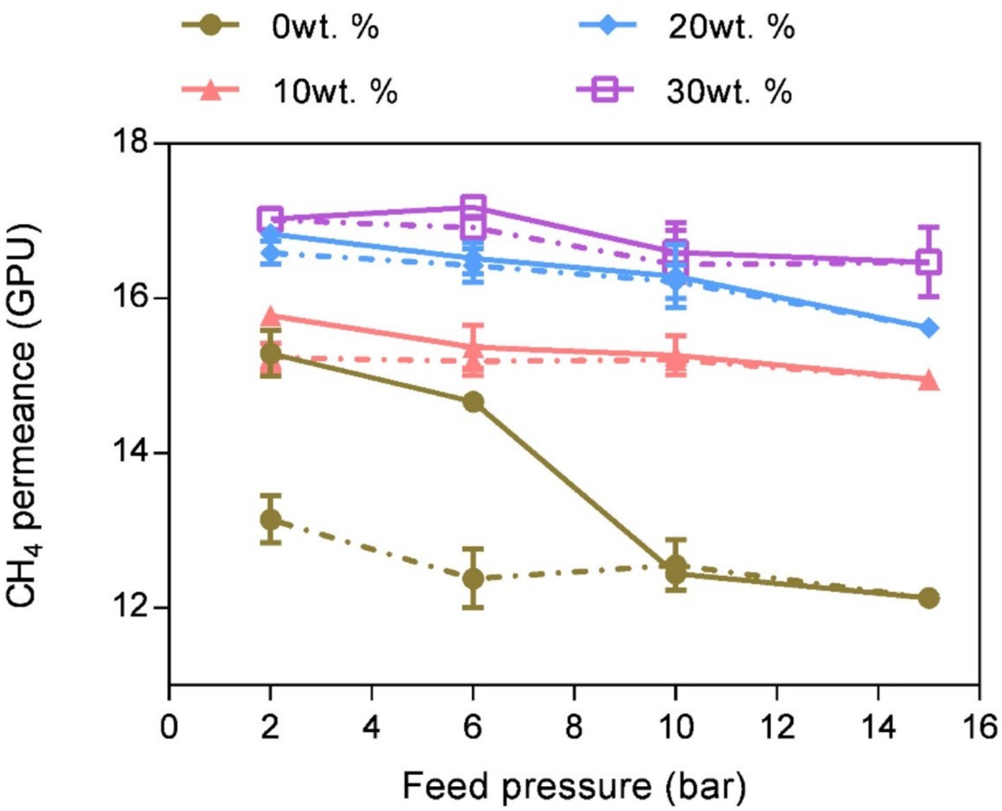

Fig.S8. CH_4 permeance at different feed pressures of ZIF-7/Pebax-1657 based composite membranes (solid line represents pressurization step and dash line represents depressurization step).